Supplementary information: Effect of electrolyte on the microstructure and yielding of aqueous dispersions of colloidal clay

Samim Ali* and Ranjini Bandyopadhyay†

Raman Research Institute, C. V. Raman Avenue,

Sadashivanagar, Bangalore 560080, India

(Dated: October 7, 2015)

* samim@rri.res.in

† ranjini@rri.res.in

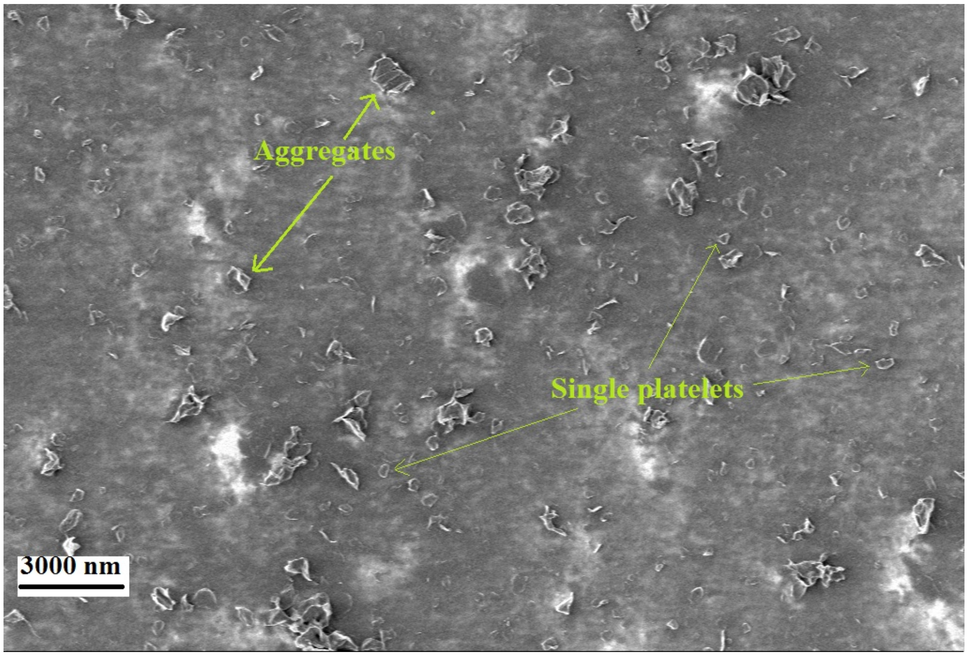

Fig. S1. SEM micrograph of Na-montmorillonite platelets and aggregates. A drop of 10 μL of 1% w/v Na-montmorillonite dispersion is spread on the hydrophilized ITO-glass plate and dried very fast (within 10 seconds) in an oven at a temperature of 200°C. The sample ITO plate is then scanned using a field effect scanning electron microscopy (ULTRA-PLUS FE-SEM) from Carl Zeiss. During the process of sample drying, the clay platelets form aggregates which can be seen in the micrograph.

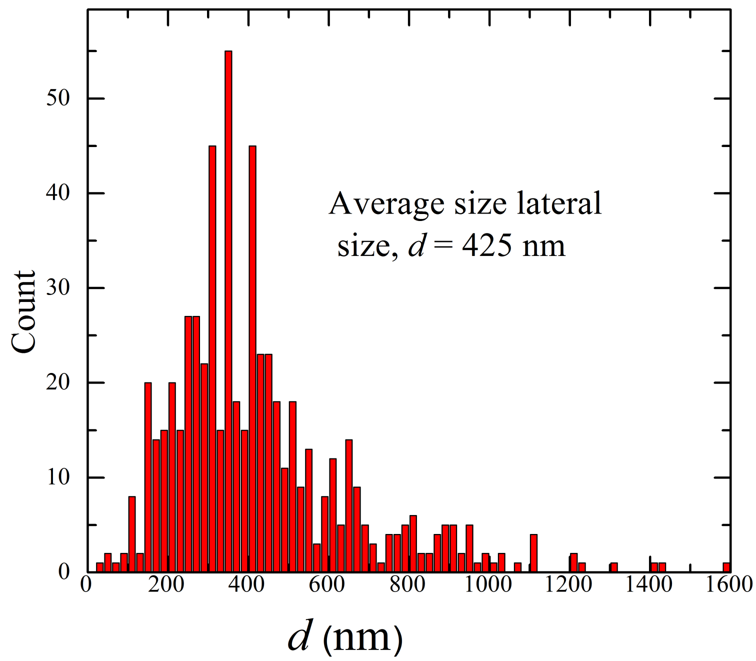

Fig. S2. Lateral size distribution of Na-montmorillonite platelets measured from SEM micrographs. Calculation of the distribution is done with 600 single platelets. The average diameter calculated from the distribution is 425 nm. Images were analyzed using ImageJ.

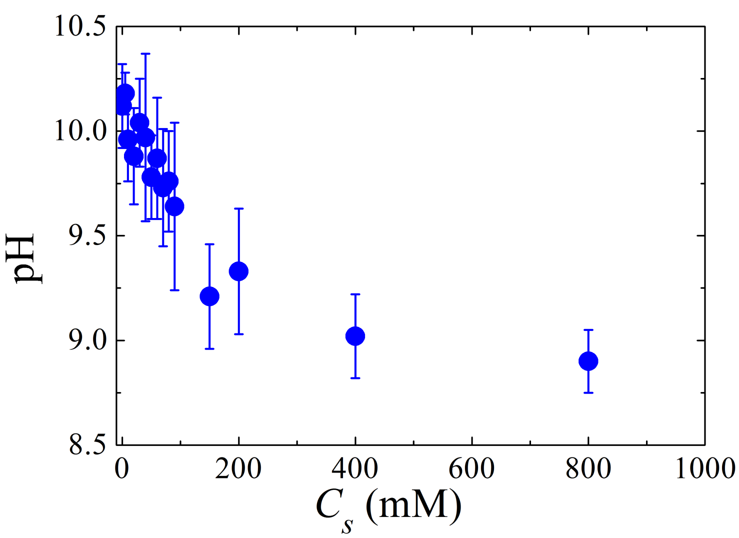

Fig. S3. Change of pH with added salt concentration C_s in freshly prepared 5% w/v Na-montmorillonite dispersions.

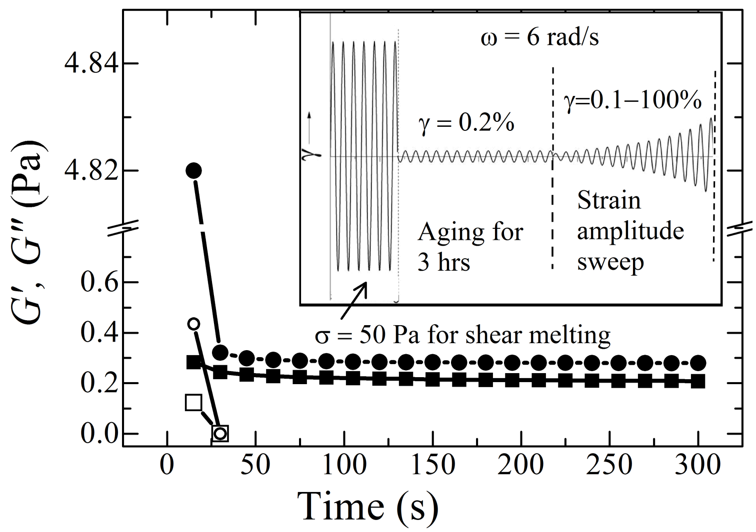

Fig. S4. Variation of the elastic modulus G' (empty symbols) and viscous modulus G'' (solid symbols) with time during the shear melting process performed by applying a stress of 50 Pa at an angular frequency of 6 rad/s for 5 mins to 5% w/v Na-montmorillonite dispersions with 20 mM (squares) and 300 mM (circles) salt concentrations. It is seen that elastic moduli of both the samples reach zero after 30 s of starting the shear melting process. Inset shows the experimental protocol used for strain amplitude sweep rheological measurements.

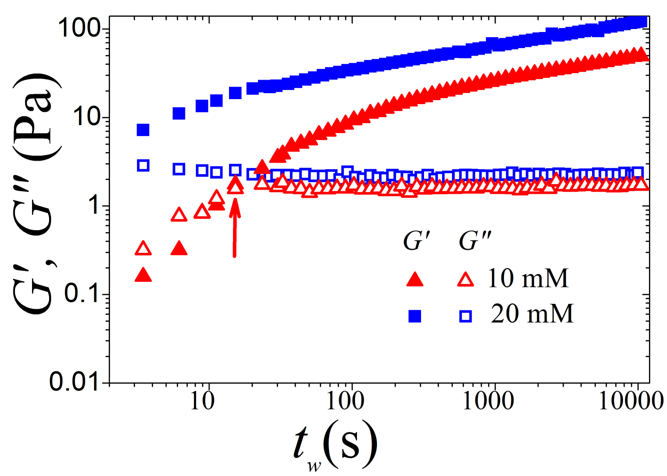

Fig. S5. Evolution of the elastic modulus G' (filled symbols) and viscous modulus G'' (empty symbols) as a function of the aging time t_w of 5% w/v Na-montmorillonite dispersions with salt concentrations 10 mM (▲ and △) and 20 mM (■ and □). The arrow shows the cross-over position between G' and G'' for the sample with 10 mM salt. To monitor the aging of the dispersions, a small oscillatory strain of amplitude $\gamma = 0.2\%$ at an angular frequency of 6 rad/s is applied to measure the t_w dependence of G' and G'' of the samples. The applied strain γ, which is very weak and much smaller than the yield strain, is not expected to interfere with the spontaneous aging process.

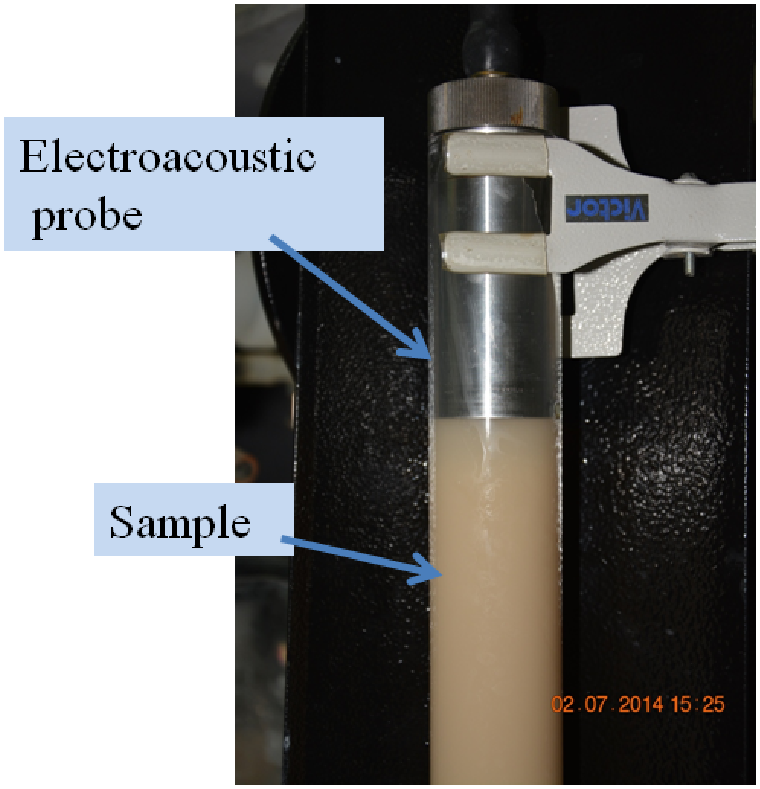

Fig. S6. Experimental setup for monitoring the sedimentation stability of clay dispersions using the electroacoustic probe. The aqueous Na-montmorillonite dispersion is loaded in a cylindrical container with inner diameter of 32.5 mm and a height of 226 mm.

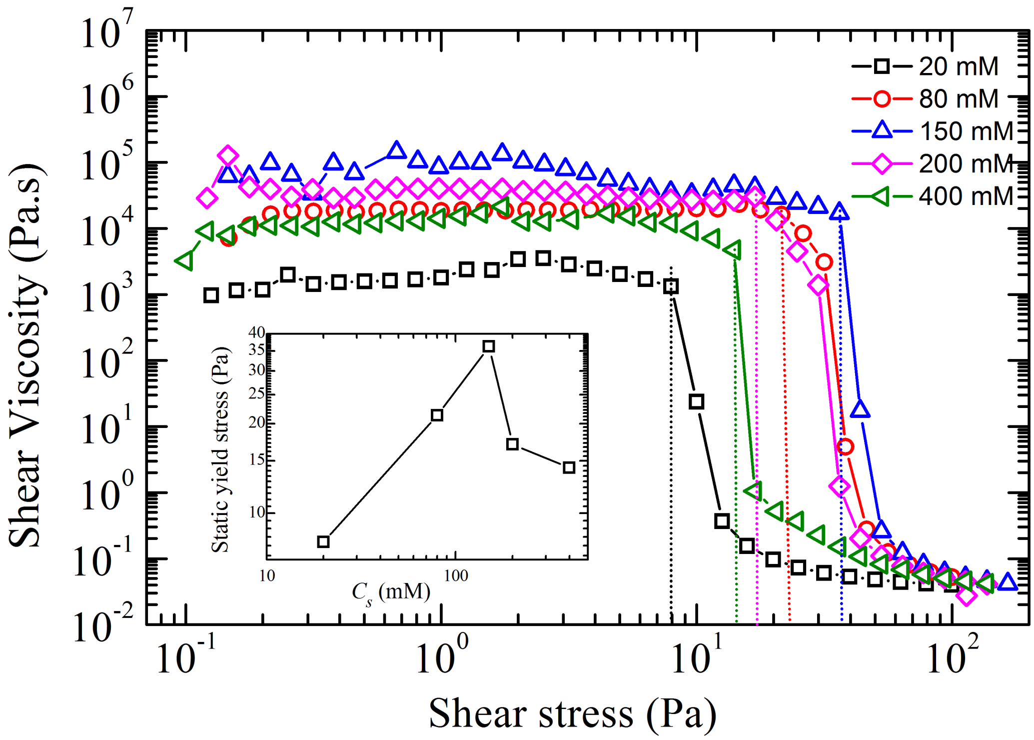

Fig. S7. Shear viscosity vs shear stress profile measured in controlled shear stress (CSS) mode for 5% w/v Na-montmorillonite dispersions with salt concentrations 20 mM (□), 80 mM (○), 150 mM (△), 200 mM (◇) and 400 mM (◁). The vertical dotted lines show the positions of the yielding points identified following the method described in ACS Appl. Mater. Interf. **3**, 3487 (2011). The inset shows the variation of static yield stress with the salt concentrations, C_s.

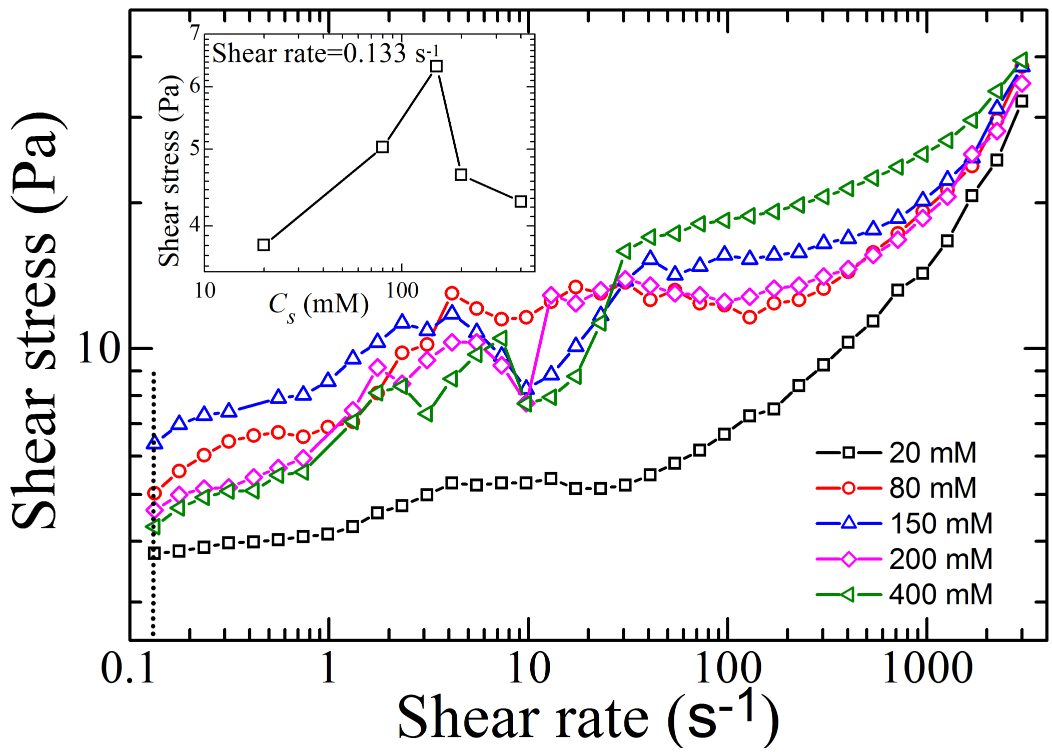

Fig. S8. Shear stress vs shear rate profile measured in controlled shear rate (CSR) mode for 5% w/v Na-montmorillonite dispersions with salt concentrations 20 mM (□), 80 mM (○), 150 mM (△), 200 mM (◇) and 400 mM (◁). Fluctuations in the shear stresses around 10 s^{-1} arise possibly due to wall slippage or a second yielding process of gels previously observed in strong gels under large deformations [Soft Matter **7**, 2456 (2011), Physical Review E **85**, 041403 (2012)]. Dynamic yield stresses are not determined due to lack of a suitable model to fit the data presented here. Instead, variation of shear stresses calculated at a low shear rate = 0.133 s^{-1} (shown by a vertical dotted line in the main plot) from the flow curves for samples with different C_s values are plotted in the inset. This also exhibit similar trend observed in Fig. 2 of main article and in the inset of Figure S7.

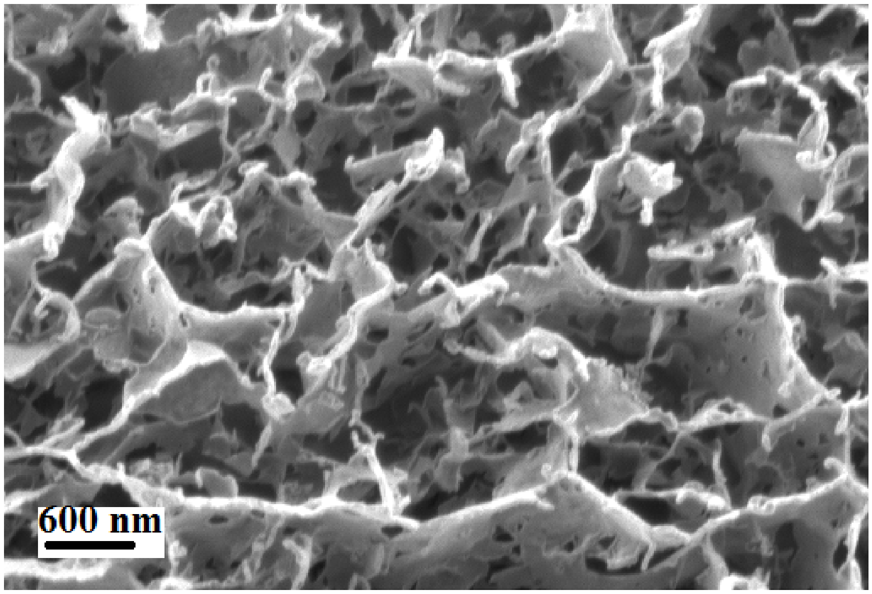

Fig. S9. Magnified cryo-SEM micrograph showing gel structure in a vitrified sample of 5% w/v Na-montmorillonite with 10 mM added salt.

A. Analysis of cryo-SEM images using ImageJ software

The cryo-SEM micrographs are analyzed using ImageJ (version: 1.49q) to calculate porosity, pore size distribution and thickness w of branches of the gel network. A cryo-SEM micrograph presents a three dimensional network structure in two dimensions with a range of pixel gray-values (intensity values). For a particular image, we manually adjust the threshold value of gray-scale using ImageJ in such a way that only the boundaries of the pores remain bright in the 2D plane. The image is then converted to binary form as shown in Figure S10. In Figure S10, the dark pixels correspond to voids spaces. Thus, the total area of dark pixels gives the total area of void spaces in the binary image. The ratio of dark area to the total area on the binary image gives the porosity value. To calculate sizes of the individual pores, each pore on the binary image is manually selected using the ImageJ pointer, as shown by a red boundary in Figure S10. The total area within this red boundary gives the pore size. The thickness (shown by green arrows in Figure S10) of a branch of network is calculated manually using the ImageJ pointer. Such measurements are repeated over several micrographs of the same sample to get good statistical averages of porosity, pore sizes and branch thickness. Figure S11 shows a representative plot of pore size distribution for a 5% w/v Na-montmorillonite gel with $C_s = 50$ mM.

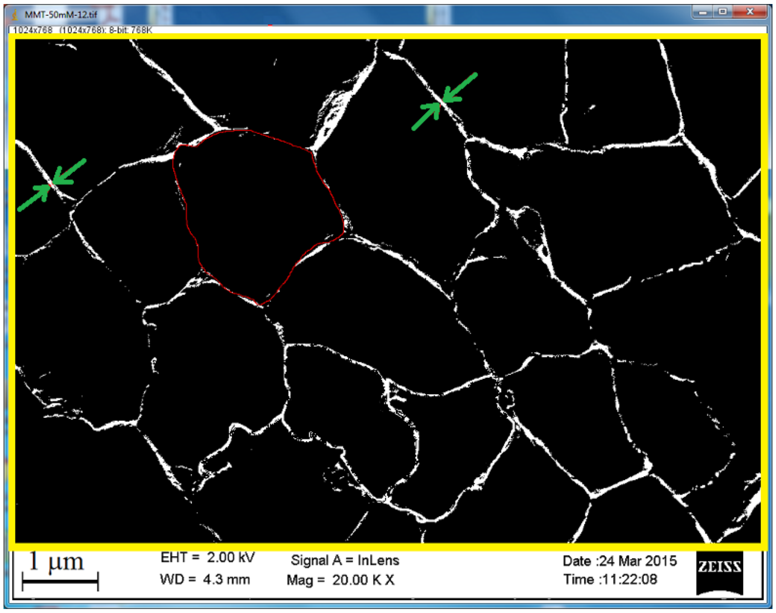

Fig. S10. A 2D projected binary image obtained using ImageJ software for a 5% w/v Na-montmorillonite gel with $C_s = 50$ mM. The details of the image processing is described in section A. The total area of the micrograph is shown by the yellow rectangle. The boundary of a pore is indicated by a closed red line. The distance between the tips of the green arrows gives the branch thickness w.

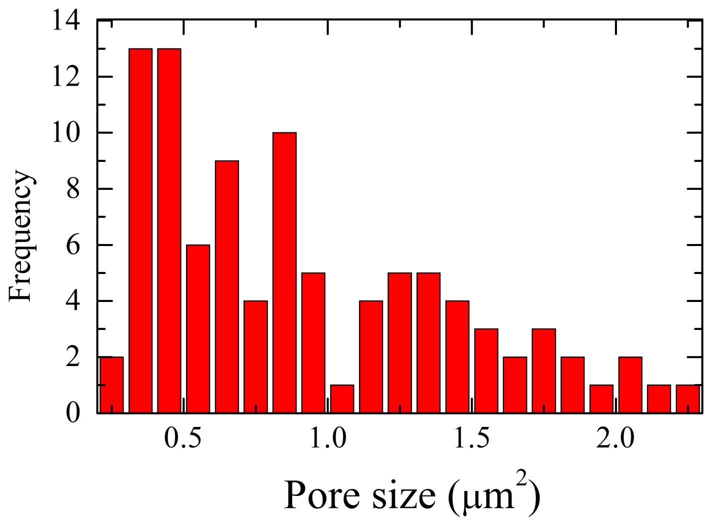

Fig. S11. A representative pore size distribution calculated from eight SEM micrographs of a 5% w/v Na-montmorillonite sample with 20 mM salt mapped on a 2D plane using ImageJ.

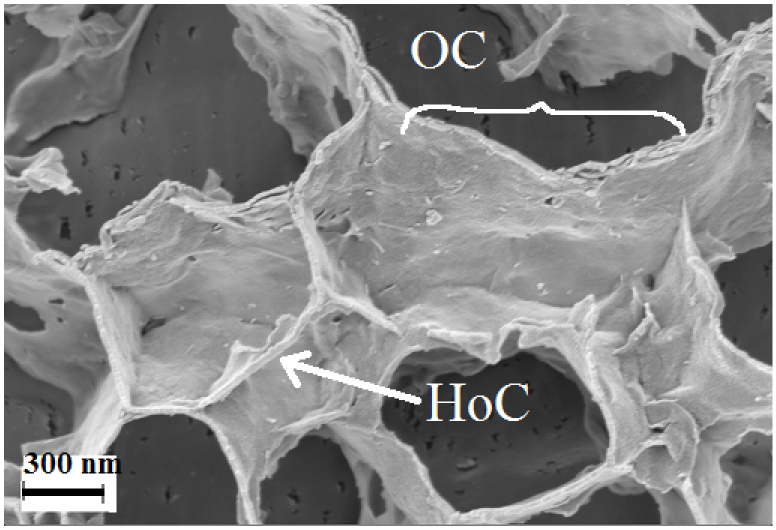

Fig. S12. Magnified cryo-SEM micrograph showing gel structures in a vitrified sample of 5% w/v Na-montmorillonite with 150 mM added salt.

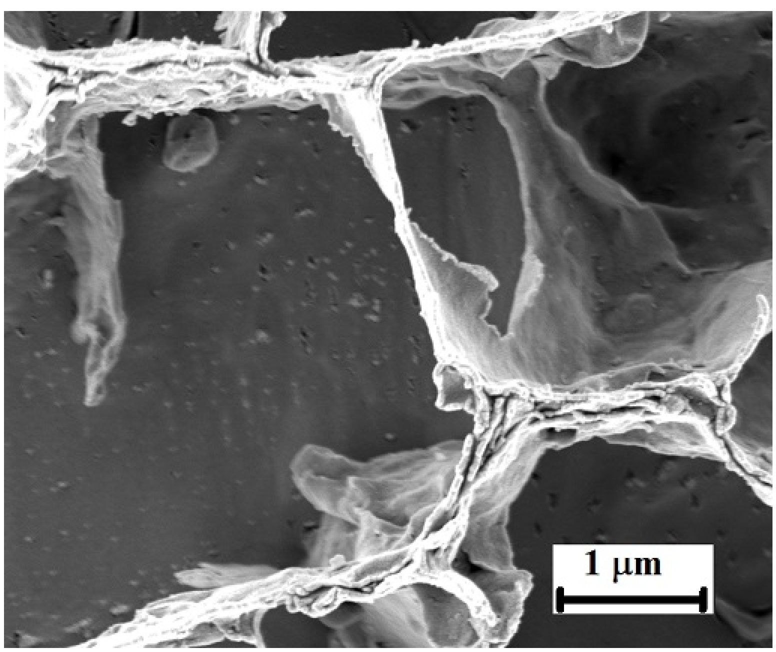

Fig. S13. Magnified cryo-SEM micrograph showing gel structures comprising overlapping coin (OC) and house of cards (HoC) configurations in a vitrified sample of 5% w/v Na-montmorillonite with 300 mM added salt.

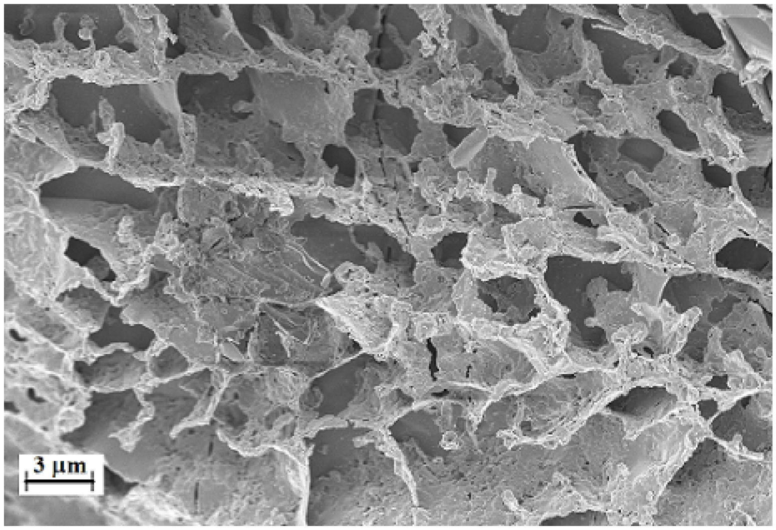

Fig. S14. SEM micrograph showing incomplete network structures in a vitrified sample of 5% w/v Na-montmorillonite with 600 mM added salt.